

# Monolithic subcell DG/FV convex property preserving scheme

**François Vilar**

Institut Montpelliérain Alexander Grothendieck, Université de Montpellier

**CFC 2023**



**UNIVERSITÉ DE  
MONTPELLIER**

**IMAG**  
INSTITUT MONPELLIERAIN  
ALEXANDER GROTHENDIECK



- 1 Introduction
- 2 DG as a subcell Finite Volume
- 3 Monolithic subcell DG/FV scheme

## Scalar conservation law

- $\partial_t u(\mathbf{x}, t) + \nabla_{\mathbf{x}} \cdot \mathbf{F}(u(\mathbf{x}, t)) = 0, \quad (\mathbf{x}, t) \in \omega \times [0, T]$
- $u(\mathbf{x}, 0) = u_0(\mathbf{x}), \quad \mathbf{x} \in \omega$

## $(k + 1)^{\text{th}}$ order semi-discretization

- $\{\omega_c\}_c$  a partition of  $\omega$ , such that  $\omega = \bigcup_c \omega_c$
- $u_h(\mathbf{x}, t)$  the numerical solution, such that  $u_h|_{\omega_c} = u_h^c \in \mathbb{P}^k(\omega_c)$

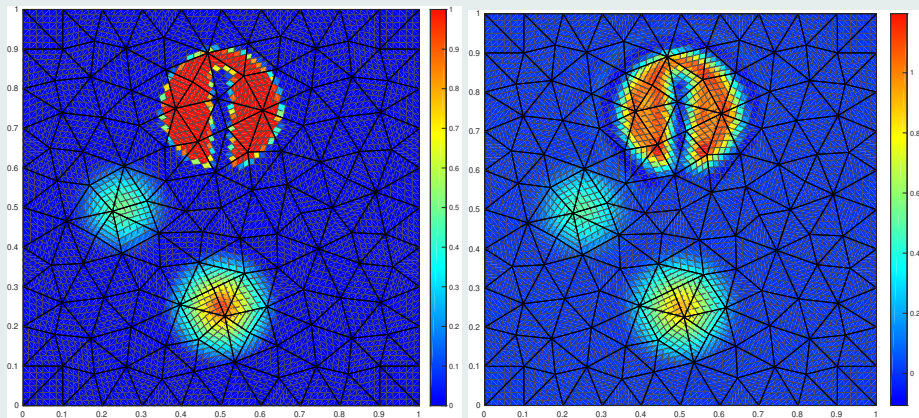
$$u_h^c(\mathbf{x}, t) = \sum_{m=1}^{N_k} u_m^c(t) \sigma_m^c(\mathbf{x})$$

- $\{\sigma_m^c\}_{m=1, \dots, N_k}$  a basis of  $\mathbb{P}^k(\omega_c)$ , with  $N_k = \frac{(k+1)(k+2)}{2}$  in 2D.

## Local variational formulation on $\omega_c$

- $\int_{\omega_c} \frac{\partial u_h^c}{\partial t} \psi \, dV = \int_{\omega_c} \mathbf{F}(u_h^c) \cdot \nabla_{\mathbf{x}} \psi \, dV - \int_{\partial \omega_c} \psi \mathcal{F}_n \, dS, \quad \forall \psi \in \mathbb{P}^k(\omega_c)$
- $\mathcal{F}_n = \mathcal{F}(u_h^c, u_h^v, \mathbf{n})$  numerical flux

# Solid body rotation: discontinuous Galerkin scheme



(a) Solution at  $t = 0$

(b) Solution at  $t = 2\pi$

**Figure :** Rotation of composite signal on 242 cells: subcells mean value

# Subcell resolution of DG scheme

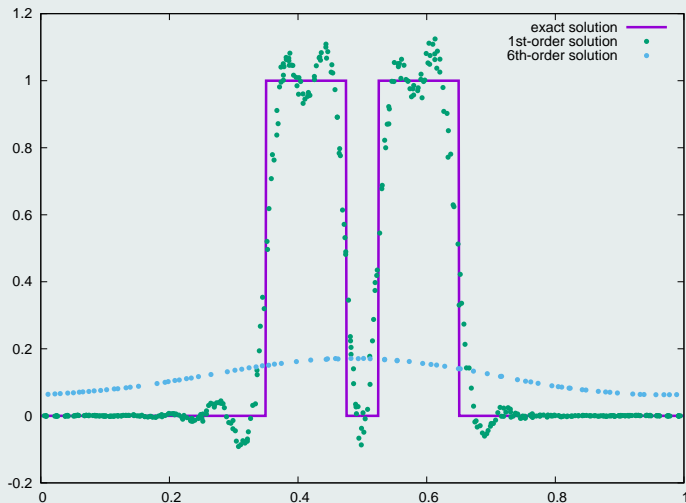


Figure : Rotation of composite signal after one period: profiles for  $y = 0.75$

## Admissible numerical solution

- Maximum principle / positivity preserving
- Ensure a correct entropic behavior

## Spurious oscillations

- Discrete maximum principle
- Relaxing condition for smooth extrema

## Methodology

**Blend, at the subcell scale, high-order DG and 1st-order FV**



**F. VILAR AND R. ABGRALL**, *A posteriori local subcell correction of DG schemes through Finite Volume reformulation on unstructured grids.* SIAM Sci. Comp., 2022. **Under revision.**



**A. RUEDA-RAMÍREZ, B. BOLM, D. KUZMIN AND G. GASSNER**, *Monolithic Convex Limiting for Legendre-Gauss-Lobatto Discontinuous Galerkin Spectral Element Methods.* Arxiv, 2023.

- 1 Introduction
- 2 DG as a subcell Finite Volume**
- 3 Monolithic subcell DG/FV scheme

# DG as a subcell Finite Volume

- Rewrite DG scheme as a FV-like scheme on a subgrid

## Cell subdivision into $N_S \geq N_k$ subcells

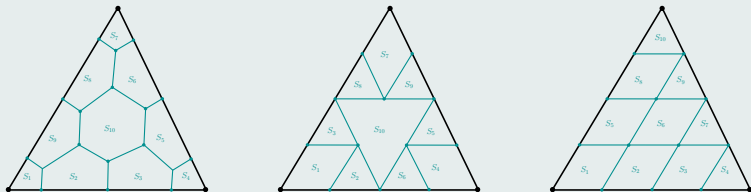


Figure : Examples of  $N_S = N_k$  subdivision for  $\mathbb{P}^3$  DG scheme on a triangle

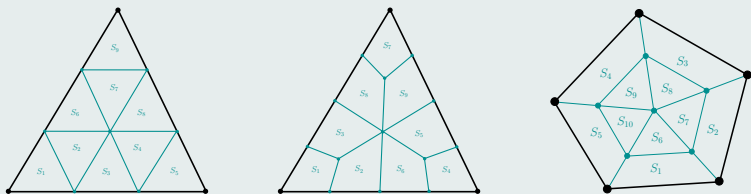


Figure : Examples of  $N_S \geq N_k$  subdivision



## DG schemes through residuals

$$\bullet \sum_{m=1}^{N_k} \frac{d u_m^c}{dt} \int_{\omega_c} \sigma_m \sigma_p dV = \int_{\omega_c} \mathbf{F}(u_h^c) \cdot \nabla_x \sigma_p dV - \int_{\partial\omega_c} \sigma_p \mathcal{F}_n dS, \quad \forall p \in \llbracket 1, N_k \rrbracket$$

$$\implies \boxed{M_c \frac{d U_c}{dt} = \Phi_c}$$

- $(U_c)_m = u_m^c$  Solution moments
- $(M_c)_{mp} = \int_{\omega_c} \sigma_m \sigma_p dV$  Mass matrix
- $(\Phi_c)_m = \int_{\omega_c} \mathbf{F}(u_h^c) \cdot \nabla_x \sigma_m dV - \int_{\partial\omega_c} \sigma_m \mathcal{F}_n dS$  DG residuals

## Subdivision and definition

- $\omega_c$  is subdivided into  $N_s$  subcells  $S_m^c$
- Let us define  $\bar{\psi}_m^c = \frac{1}{|S_m^c|} \int_{S_m^c} \psi dV$  the subcell mean value

## Submean values

$$\bullet \bar{u}_m^c = \frac{1}{|S_m^c|} \sum_{q=1}^{N_k} u_q^c \int_{S_m^c} \sigma_q dV \quad \Rightarrow \quad \boxed{\bar{U}_c = P_c U_c}$$

$$\bullet (\bar{U}_c)_m = \bar{u}_m^c \quad \text{Submean values}$$

$$\bullet (P_c)_{mp} = \frac{1}{|S_m^c|} \int_{S_m^c} \sigma_p dV \quad \text{Projection matrix}$$

$$\Rightarrow \quad \boxed{\frac{d\bar{U}_c}{dt} = P_c M_c^{-1} \Phi_c}$$

## Admissibility of the cell sub-partition into subcells

$$\bullet P_c^t P_c \quad \text{has to be non-singular}$$

$$\Rightarrow \quad \boxed{U_c = (P_c^t P_c)^{-1} P_c^t \bar{U}_c} \quad \text{Least square procedure}$$

$$\bullet \text{ If } N_s = N_k, \quad \bar{U}_c = P_c U_c \iff U_c = P_c^{-1} \bar{U}_c$$

## Subcell Finite Volume: reconstructed fluxes

- Let us introduce the **reconstructed fluxes** such that

$$\frac{d\bar{u}_m^c}{dt} = -\frac{1}{|S_m^c|} \int_{\partial S_m^c} \widehat{F}_n dS$$

- Let  $\mathcal{V}_m^c$  be the set of face neighboring subcells of  $S_m^c$

$$\frac{d\bar{u}_m^c}{dt} = -\frac{1}{|S_m^c|} \sum_{S_p^v \in \mathcal{V}_m^c} \int_{f_{mp}^c} \widehat{F}_n dS$$

- We impose that on the boundary of cell  $\omega_c$

$$\widehat{F}_n|_{\partial\omega_c} = \mathcal{F}_n$$

- Then, if  $\widetilde{\mathcal{V}}_m^c$  stands for the set of face neighboring subcells inside  $\omega_c$

$$\frac{d\bar{u}_m^c}{dt} = -\frac{1}{|S_m^c|} \left( \sum_{S_p^v \in \widetilde{\mathcal{V}}_m^c} \int_{f_{mp}^c} \widehat{F}_n dS + \int_{\partial S_m^c \cap \partial\omega_c} \mathcal{F}_n dS \right)$$

# Subcell Finite Volume: reconstructed fluxes

- Taking two subcells  $S_m^c$  and  $S_p^v$ , the orientation face function  $\varepsilon_{mp}^c$  writes

$$\varepsilon_{mp}^c = \begin{cases} 1 & \text{if face } f_{mp}^c \text{ is direct or if } f_{mp}^c \subset \partial\omega_c, \\ -1 & \text{if face } f_{mp}^c \text{ is indirect,} \\ 0 & \text{if } S_p^v \notin \mathcal{V}_m^c. \end{cases}$$

- $\int_{f_{mp}^c} \widehat{F}_n \, dS := \widehat{F}_{mp} = -\widehat{F}_{pm}$  face integrated reconstructed flux

$$\frac{d\bar{U}_m^c}{dt} = -\frac{1}{|S_m^c|} \left( \sum_{S_p^v \in \widetilde{\mathcal{V}}_m^c} \widehat{F}_{mp} + \int_{\partial S_m^c \cap \partial\omega_c} \mathcal{F}_n \, dS \right)$$

- $(B_c)_m = \int_{\partial S_m^c \cap \partial\omega_c} \mathcal{F}_n \, dS$  Cell boundary contribution
- $(A_c)_{mp} = \varepsilon_{mp}^c$  Adjacency matrix
- $D_c = \text{diag}(|S_1^c|, \dots, |S_{N_k}^c|)$  Subcells volume matrix

## Subcell Finite Volume: reconstructed fluxes

- Let  $\widehat{F}_c$  be the vector containing all the interior faces reconstructed fluxes
- The subcell mean values governing equations yield the following system

$$-A_c \widehat{F}_c = D_c \frac{d\bar{U}_c}{dt} + B_c$$

## Graph Laplacian technique

- $A_c \in \mathcal{M}_{N_s \times N_f^c}$  with  $N_f^c$  the number of interior faces
- $A_c^t \mathbf{1} = \mathbf{0}$  where  $\mathbf{1} = (1, \dots, 1)^t \in \mathbb{R}^{N_s}$



**R. ABGRALL**, *Some Remarks about Conservation for Residual Distribution Schemes*. *Methods Appl. Math.*, 18:327-351, 2018.

- Let  $\mathcal{L}_c^{-1}$  be the inverse of  $L_c = A_c A_c^t$  on the orthogonal of its kernel

$$\mathcal{L}_c^{-1} = (L_c + \lambda \Pi)^{-1} - \frac{1}{\lambda} \Pi$$

$$\forall \lambda \neq 0$$

- $\Pi = \frac{1}{N_s} (\mathbf{1} \otimes \mathbf{1}) \in \mathcal{M}_{N_s}$

## Graph Laplacian technique

- Finally, we obtain the following definition of the reconstructed fluxes

$$\widehat{F}_c = -A_c^t \mathcal{L}_c^{-1} \left( D_c P_c M_c^{-1} \Phi_c + B_c \right)$$

### remark

- The only terms depending on the time are  $\Phi_c$  and  $B_c$

### One-dimensional case: $N_f^i = N_s - 1$



$$A_i = \begin{pmatrix} 1 & 0 & \dots & 0 \\ -1 & 1 & \ddots & \vdots \\ 0 & \ddots & \ddots & \vdots \\ \vdots & \ddots & \ddots & 1 \\ 0 & \dots & \dots & -1 \end{pmatrix}, \quad L_i = A_i A_i^t = \begin{pmatrix} 1 & -1 & 0 & \dots & 0 \\ -1 & 2 & 1 & \ddots & \vdots \\ 0 & \ddots & \ddots & \ddots & \vdots \\ \vdots & \dots & -1 & 2 & 1 \\ 0 & \dots & 0 & -1 & 1 \end{pmatrix}$$

$$B_i = \left( -\mathcal{F}_{i-\frac{1}{2}}, 0, \dots, 0, \mathcal{F}_{i+\frac{1}{2}} \right)^t$$

# Different cell subdivisions

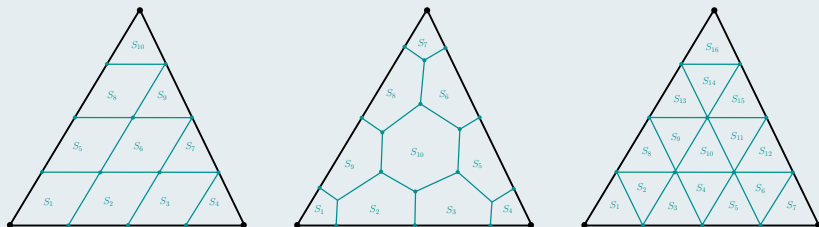
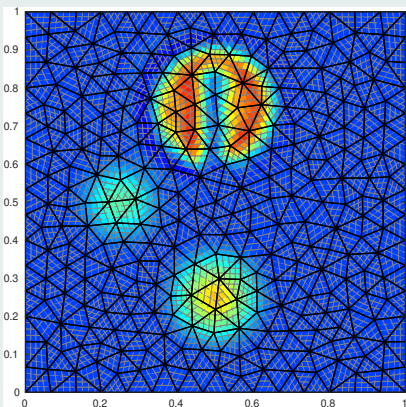


Figure : Examples of easily generalizable subdivisions for a triangle cell

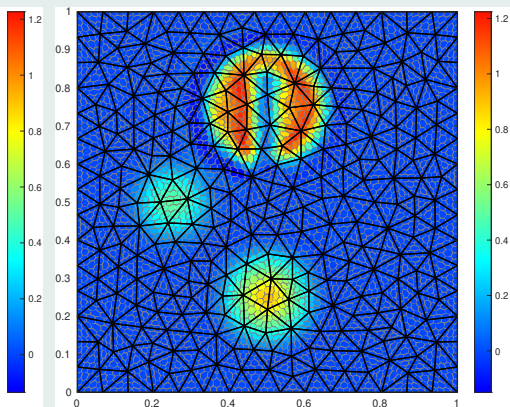
## DG is DG

- Only the functional space matters
- The cell subdivision has no influence on the resulting scheme
- Even in the case where  $N_s > N_k$

# Rotation of a composite signal after one full rotation



(a) Cartesian subdivision

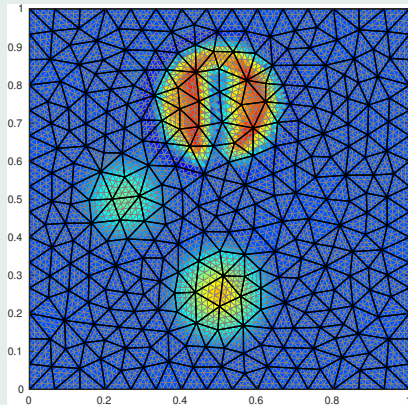


(b) Polygonal subdivision

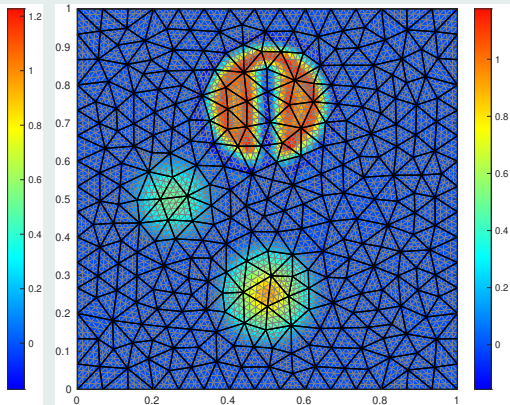
Figure :  $\mathbb{P}^3$  reconstructed flux FV schemes on 576 cells: subcells mean values



# Rotation of a composite signal after one full rotation



(a) Triangular subdivision



(b) Enriched-DG triangular subdivision

Figure :  $\mathbb{P}^3$  and  $\mathbb{P}^{4+\frac{1}{6}}$  reconstructed flux FV schemes on 576 cells: subcells mean values

# Rotation of a composite signal after one full rotation

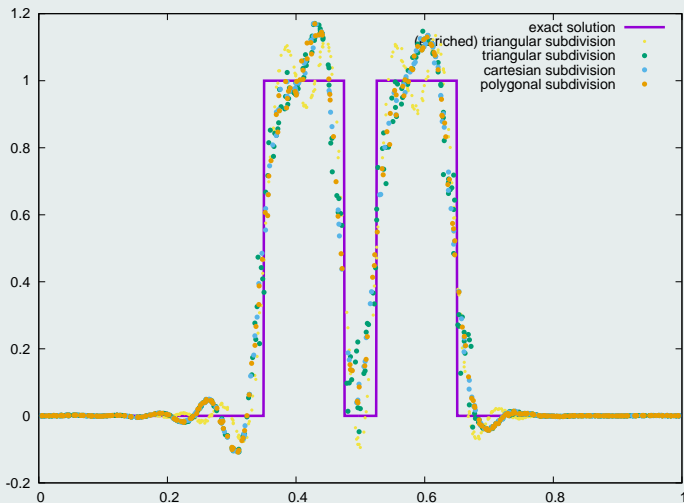
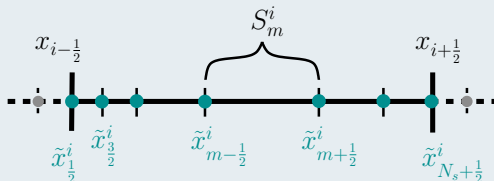


Figure : Reconstructed flux FV schemes on 576 cells: solution profiles for  $y = 0.75$

- 1 Introduction
- 2 DG as a subcell Finite Volume
- 3 Monolithic subcell DG/FV scheme**

## Definitions

$$\bar{u}_0^i := \bar{u}_{N_s}^{i-1} \quad \text{and} \quad \bar{u}_{N_s+1}^i := \bar{u}_1^{i+1}$$



$$\bullet \widehat{F}_{m+\frac{1}{2}}^i$$

high-order reconstructed flux

$$\bullet \mathcal{F}_{m+\frac{1}{2}}^i := \mathcal{F}(\bar{u}_m^i, \bar{u}_{m+1}^i)$$

first-order subcell numerical flux

$$= \frac{F(\bar{u}_m^i) + F(\bar{u}_{m+1}^i)}{2} - \frac{\gamma_{m+\frac{1}{2}}}{2} (\bar{u}_{m+1}^i - \bar{u}_m^i)$$

**E-flux**

$$\bullet \widetilde{F}_{m+\frac{1}{2}}^i := \mathcal{F}_{m+\frac{1}{2}}^i + \theta_{m+\frac{1}{2}}^i \underbrace{\left( \widehat{F}_{m+\frac{1}{2}}^i - \mathcal{F}_{m+\frac{1}{2}}^i \right)}_{\Delta F_{m+\frac{1}{2}}^i}$$

convex blended flux

## Remarks

- We drop superscript  $i$ , as the cell structure is only seen in the construction of the reconstructed fluxes  $\widetilde{F}_{m+\frac{1}{2}}^i$
- We focus on forward Euler (FE) time stepping, as SSP Runge-Kutta can be formulated as convex combinations of FE
- We drop superscript  $n$  when not explicitly needed

## Reformulation of the monolithic subcell scheme

$$\begin{aligned}
 \bullet \quad \bar{u}_m^{n+1} &= \bar{u}_m - \frac{\Delta t}{|S_m|} \left( \widetilde{F}_{m+\frac{1}{2}} - \widetilde{F}_{m-\frac{1}{2}} \right) \pm F(\bar{u}_m) \pm \frac{\Delta t}{|S_m|} \left( \gamma_{m+\frac{1}{2}} + \gamma_{m-\frac{1}{2}} \right) \\
 &= \left( 1 - \frac{\Delta t}{|S_m|} \left( \gamma_{m+\frac{1}{2}} + \gamma_{m-\frac{1}{2}} \right) \right) \bar{u}_m \\
 &+ \frac{\Delta t}{|S_m|} \gamma_{m+\frac{1}{2}} \underbrace{\left( \bar{u}_m - \frac{\widetilde{F}_{m+\frac{1}{2}} - F(\bar{u}_m)}{\gamma_{m+\frac{1}{2}}} \right)}_{\widetilde{u}_{m+\frac{1}{2}}^-} + \frac{\Delta t}{|S_m|} \gamma_{m-\frac{1}{2}} \underbrace{\left( \bar{u}_m + \frac{\widetilde{F}_{m-\frac{1}{2}} - F(\bar{u}_m)}{\gamma_{m-\frac{1}{2}}} \right)}_{\widetilde{u}_{m-\frac{1}{2}}^+}
 \end{aligned}$$

## Convex combination

- $\lambda_{m\pm\frac{1}{2}} = \frac{\Delta t}{|S_m|} \gamma_{m\pm\frac{1}{2}}$

$$\bar{u}_m^{n+1} = \left(1 - (\lambda_{m-\frac{1}{2}} + \lambda_{m+\frac{1}{2}})\right) \bar{u}_m + \lambda_{m+\frac{1}{2}} \widetilde{u}_{m+\frac{1}{2}}^- + \lambda_{m-\frac{1}{2}} \widetilde{u}_{m-\frac{1}{2}}^+$$

- $\Delta t \leq \frac{|S_m|}{\gamma_{m-\frac{1}{2}} + \gamma_{m+\frac{1}{2}}}$

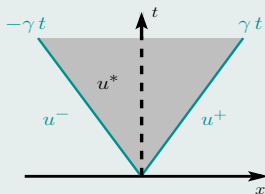
CFL condition

## Modified Riemann intermediate states

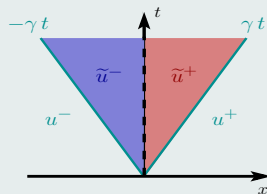
- $$\begin{aligned} \widetilde{u}_{m+\frac{1}{2}}^- &= \bar{u}_m - \frac{\widetilde{F}_{m+\frac{1}{2}} - F(\bar{u}_m)}{\gamma_{m+\frac{1}{2}}} = \bar{u}_m - \frac{\mathcal{F}_{m+\frac{1}{2}} - F(\bar{u}_m)}{\gamma_{m+\frac{1}{2}}} - \theta_{m+\frac{1}{2}} \frac{\Delta F_{m+\frac{1}{2}}}{\gamma_{m+\frac{1}{2}}} \\ &= \underbrace{\frac{\bar{u}_m + \bar{u}_{m+1}}{2} - \frac{F(\bar{u}_{m+1}) - F(\bar{u}_m)}{2\gamma_{m+\frac{1}{2}}}}_{u_{m+\frac{1}{2}}^*} - \theta_{m+\frac{1}{2}} \frac{\Delta F_{m+\frac{1}{2}}}{\gamma_{m+\frac{1}{2}}} \end{aligned}$$

## Modified Riemann intermediate states

$$\bullet \widetilde{u}_{m+\frac{1}{2}}^{\pm} = u_{m+\frac{1}{2}}^* \pm \theta_{m+\frac{1}{2}} \frac{\Delta F_{m+\frac{1}{2}}}{\gamma_{m+\frac{1}{2}}} \implies u_{m+\frac{1}{2}}^* = \frac{1}{2} \left( \widetilde{u}_{m+\frac{1}{2}}^{-} + \widetilde{u}_{m+\frac{1}{2}}^{+} \right)$$



(a) 1st-order situation



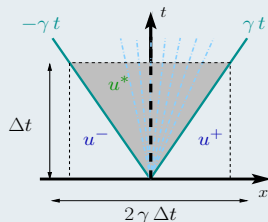
(b) Blended flux situation

## Weak entropic solution average

$$\bullet u^* := \frac{u^- + u^+}{2} - \frac{F(u^+) - F(u^-)}{2\gamma}$$

$$= \frac{1}{2\gamma\Delta t} \int_{-\gamma\Delta t}^{\gamma\Delta t} \mathcal{W}\left(\frac{x}{\Delta t}; u^-, u^+\right) dx$$

$$\bullet \gamma \geq \max_{u \in I(u^-, u^+)} |F'(u)|$$



## Global maximum principle

$$\bar{u}_m^{n+1} \in [\alpha, \beta]$$

$$\theta_{m+\frac{1}{2}} \leq \min \left( 1, \underbrace{\left| \frac{\gamma_{m+\frac{1}{2}}}{\Delta F_{m+\frac{1}{2}}} \right|}_{D_{m+\frac{1}{2}}} \min \left( \beta - u_{m+\frac{1}{2}}^*, u_{m+\frac{1}{2}}^* - \alpha \right) \right)$$

## Local maximum principle

$$\bar{u}_m^{n+1} \in I(\bar{u}_{m-1}^n, \bar{u}_m^n, \bar{u}_{m+1}^n)$$

- $\widetilde{u}_{m+\frac{1}{2}}^- \in [\alpha_m, \beta_m] := I(\bar{u}_{m-1}^n, \bar{u}_m^n, \bar{u}_{m+1}^n)$
- $\widetilde{u}_{m+\frac{1}{2}}^+ \in [\alpha_{m+1}, \beta_{m+1}] := I(\bar{u}_m^n, \bar{u}_{m+1}^n, \bar{u}_{m+2}^n)$

$$\theta_{m+\frac{1}{2}} \leq \min \left( 1, |D_{m+\frac{1}{2}}| \begin{cases} \min(\beta_{m+1} - u_{m+\frac{1}{2}}^*, u_{m+\frac{1}{2}}^* - \alpha_m) & \text{if } \Delta F_{m+\frac{1}{2}} > 0 \\ \min(\beta_m - u_{m+\frac{1}{2}}^*, u_{m+\frac{1}{2}}^* - \alpha_{m+1}) & \text{if } \Delta F_{m+\frac{1}{2}} < 0 \end{cases} \right)$$

- Smooth extrema relaxation to preserve accuracy



# Linear advection of a composite signal

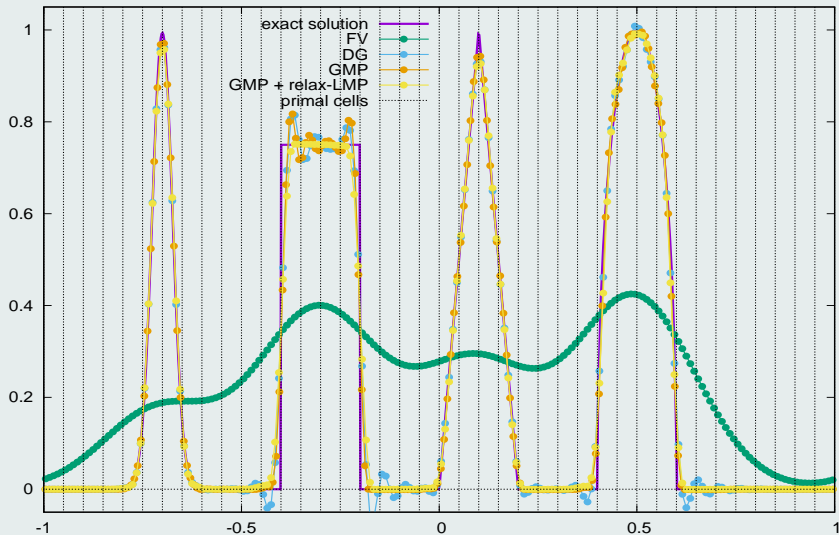
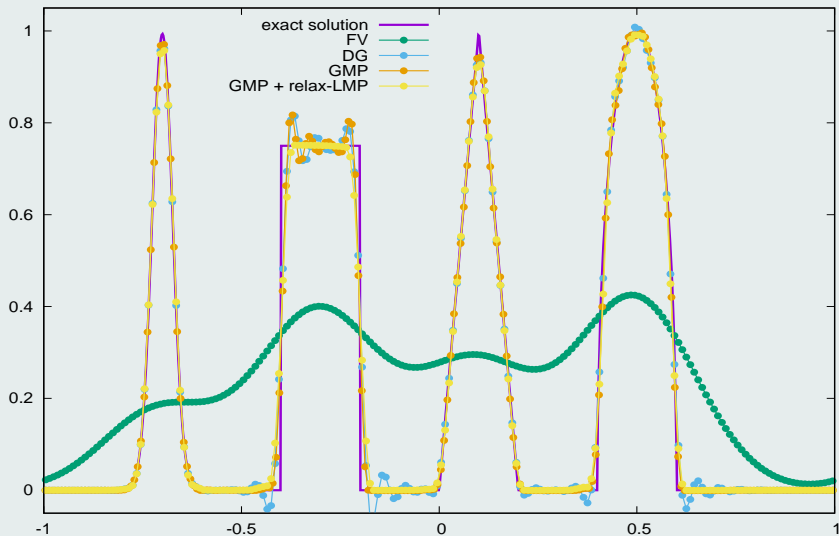
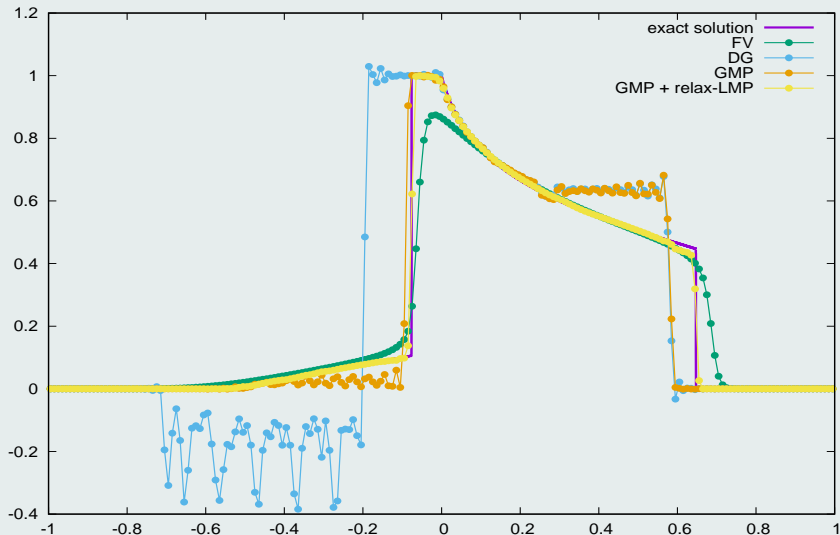


Figure :  $\mathbb{P}^5$ -DG/FV solutions on 40 cells: submean values

## Linear advection of a composite signal

Figure :  $\mathbb{P}^5$ -DG/FV solutions on 40 cells: submean values

## Non-linear non-convex flux Buckley case

Figure :  $\mathbb{P}^4$ -DG/FV solutions on 40 cells: submean values

## Definitions

- $(\eta, \phi)$  entropy - entropy flux
- $v(u) = \eta'(u)$  entropy variable
- $\psi(u) = v(u) F(u) - \phi(u)$  entropy potential
- $\phi^*(u^-, u^+) = \frac{\phi(u^-) + \phi(u^+)}{2} - \frac{\gamma}{2} (\eta(u^+) - \eta(u^-))$
- $\eta(u^*) \leq \eta^* := \frac{\eta(u^-) + \eta(u^+)}{2} - \frac{\eta(u^+) - \eta(u^-)}{2\gamma}$

## Subcell entropy stability at the discrete level

for all  $(\eta, \phi)$

- if  $\Delta F_{m+\frac{1}{2}} \cdot (\bar{u}_{m+1} - \bar{u}_m) > 0$ ,

$$\theta_{m+\frac{1}{2}} \leq \min \left( 1, \frac{(\gamma_{m+\frac{1}{2}} - \gamma_{\text{God}}) (\bar{u}_{m+1} - \bar{u}_m)}{2 \Delta F_{m+\frac{1}{2}}} \right)$$

- $\gamma_{\text{God}}$  Godunov viscosity coefficient

# Subcell entropy stability at the discrete level for a given $(\eta, \phi)$

- if  $\Delta F_{m+\frac{1}{2}} \cdot v \left( u_{m+\frac{1}{2}}^* + \frac{1}{D_{m+\frac{1}{2}}} \right) > 0$ ,

$$\theta_{m+\frac{1}{2}} \leq \min \left( 1, \frac{(\eta_{m+\frac{1}{2}}^* - \eta(u_{m+\frac{1}{2}}^*)) |D_{m+\frac{1}{2}}|}{|v(u_{m+\frac{1}{2}}^* + \frac{1}{D_{m+\frac{1}{2}}})|} \right)$$

- if  $\Delta F_{m+\frac{1}{2}} \cdot v \left( u_{m+\frac{1}{2}}^* - \frac{1}{D_{m+\frac{1}{2}}} \right) < 0$ ,

$$\theta_{m+\frac{1}{2}} \leq \min \left( 1, \frac{(\eta_{m+\frac{1}{2}}^* - \eta(u_{m+\frac{1}{2}}^*)) |D_{m+\frac{1}{2}}|}{|v(u_{m+\frac{1}{2}}^* - \frac{1}{D_{m+\frac{1}{2}}})|} \right)$$

## Subcell entropy conservation/dissipation at the semi-discrete level for a given $(\eta, \phi)$

- if  $\Delta F_{m+\frac{1}{2}} \cdot (v(\bar{u}_{m+1}) - v(\bar{u}_m)) > 0$ ,

$$\theta_{m+\frac{1}{2}} \leq \min \left( 1, \frac{\frac{\psi(\bar{u}_{m+1}) - \psi(\bar{u}_m)}{v(\bar{u}_{m+1}) - v(\bar{u}_m)} - \mathcal{F}_{m+\frac{1}{2}}}{\Delta F_{m+\frac{1}{2}}} \right)$$



**D. KUZMIN AND M. QUEZADA DE LUNA**, *Algebraic entropy fixes and convex limiting for continuous finite element discretizations of scalar hyperbolic conservation laws*. *Comp. Math. Appl. Mech. Eng.*, 2020.



**A. RUEDA-RAMÍREZ, B. BOLM, D. KUZMIN AND G. GASSNER**, *Monolithic Convex Limiting for Legendre-Gauss-Lobatto Discontinuous Galerkin Spectral Element Methods*. *Arxiv*, 2023.

# Cell entropy conservation/dissipation at the semi-discrete level for a given $(\eta, \phi)$

- if  $\Delta F_{m+\frac{1}{2}} \cdot (\underline{v}_{m+1} - \underline{v}_m) > 0$ ,

$$\theta_{m+\frac{1}{2}} \leq \min \left( 1, \frac{\frac{\psi(u(\underline{v}_{m+1})) - \psi(u(\underline{v}_m))}{\underline{v}_{m+1} - \underline{v}_m} - \mathcal{F}_{m+\frac{1}{2}}}{\Delta F_{m+\frac{1}{2}}} \right)$$

- $\mathcal{F}_{m+\frac{1}{2}} := \mathcal{F}(u(\underline{v}_{m+1}), u(\underline{v}_m))$  modified FV numerical flux
- $v_h^i = \sum_{m=1}^{k+1} \underline{v}_m^i \varphi_m^i \in \mathbb{P}^k$   $L^2$  projection of  $v(u_h^i)$  onto  $\mathbb{P}^k$
- $\{\varphi_m^i\}_{m=1, \dots, k+1}$   $L^2$  projection of  $\{\mathbb{1}_{S_m^i}\}_m$  onto  $\mathbb{P}^k$

# Linear advection of a composite signal

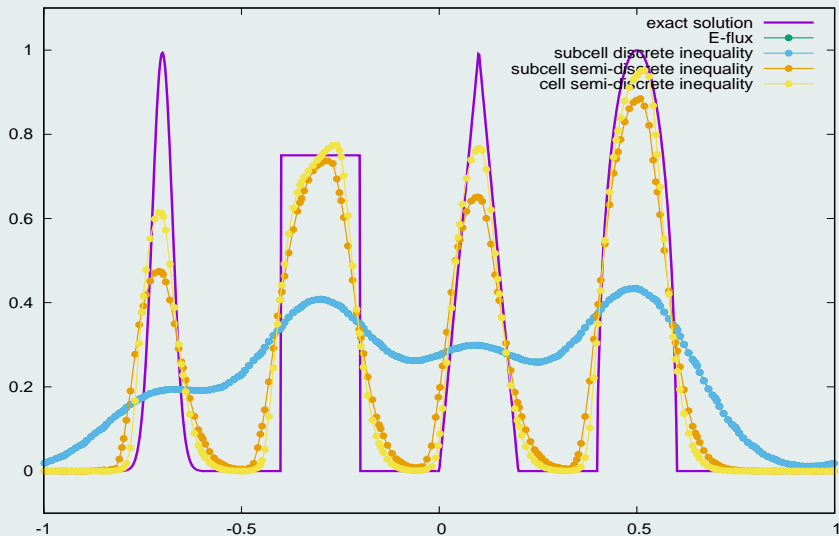


Figure :  $\mathbb{P}^5$ -DG/FV solutions on 40 cells: submean values



# Linear advection of a composite signal

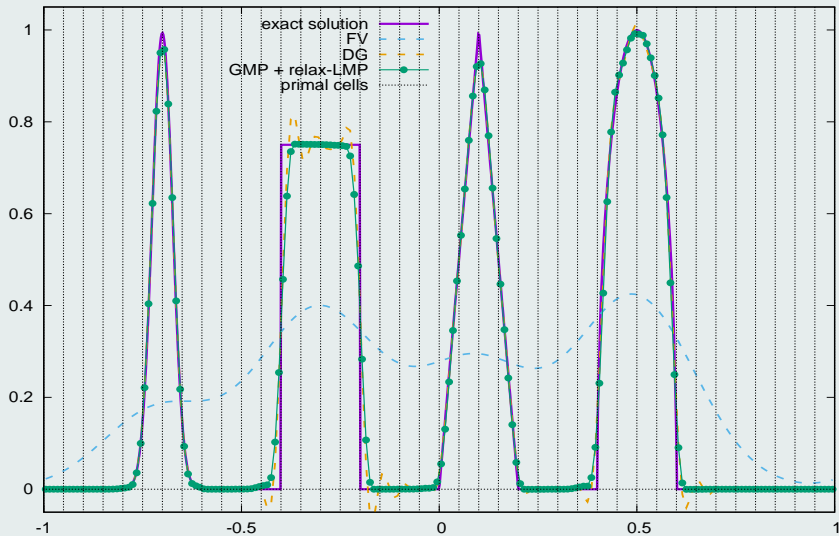


Figure :  $\mathbb{P}^4$ -DG/FV solutions on 40 cells: submean values

# Non-linear non-convex flux Buckley case

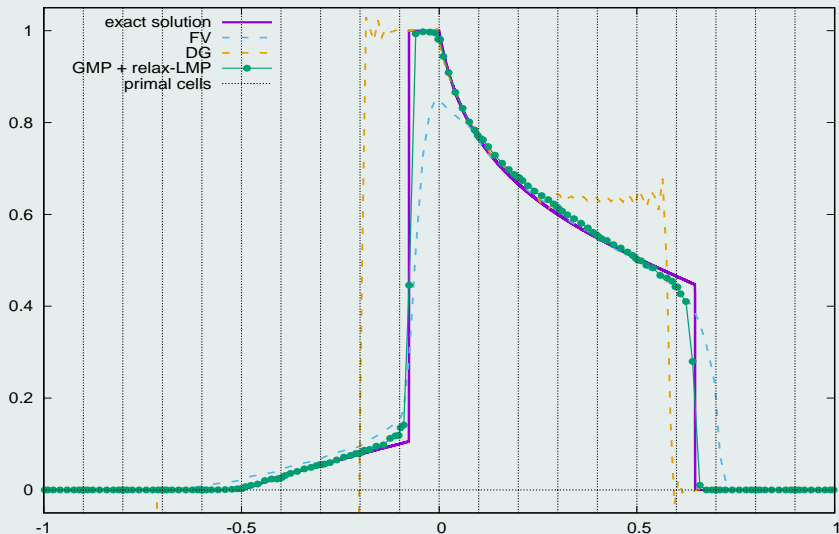
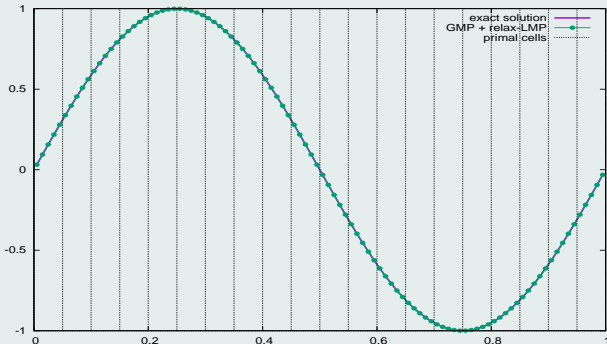


Figure :  $\mathbb{P}^7$ -DG/FV solutions on 20 cells: submean values

## Linear advection of a smooth function

$$u_0(x) = \sin(2\pi x)$$



$h$	$L_1$		$L_2$	
	$E_{L_1}^h$	$q_{L_1}^h$	$E_{L_2}^h$	$q_{L_2}^h$
$\frac{1}{20}$	2.63E-8	4.97	3.29E-8	4.98
$\frac{1}{40}$	8.39E-10	5.08	1.04E-9	5.04
$\frac{1}{80}$	2.47E-11	-	3.16E-11	-

**Table:** Convergence rates for the linear advection case with a 5th-order DG/FV scheme

# Non-linear Euler compressible gas dynamics equations

- $\partial_t \mathbf{V} + \nabla_x \cdot \mathbf{F}(\mathbf{V}) = \mathbf{0}$

- $\mathbf{V} = \begin{pmatrix} \rho \\ \mathbf{q} \\ E \end{pmatrix}$

conservative variables

- $\mathbf{F}(\mathbf{V}) = \begin{pmatrix} \mathbf{q} \\ \frac{\mathbf{q} \otimes \mathbf{q}}{\rho} + p I_d \\ (E + p) \frac{\mathbf{q}}{\rho} \end{pmatrix}$

flux function

- $p := p(\mathbf{V}) = (\gamma - 1) \left( E - \frac{1}{2} \frac{\|\mathbf{q}\|^2}{\rho} \right)$

equation of state

## Monolithic subcell DG/FV scheme property

- Positivity of the density and internal energy, at the subcell scale

## Definitions

- $$\widehat{\mathbf{F}}_{m+\frac{1}{2}} := \mathbf{F}_{m+\frac{1}{2}} + \Theta_{m+\frac{1}{2}} \underbrace{(\mathbf{F}_{m+\frac{1}{2}} - \mathbf{F}_{m+\frac{1}{2}})}_{\Delta \mathbf{F}_{m+\frac{1}{2}}}$$

convex blended flux

- $$\Theta_{m+\frac{1}{2}} = \begin{pmatrix} \theta_{m+\frac{1}{2}}^\rho & 0 & 0 \\ 0 & \theta_{m+\frac{1}{2}}^q & 0 \\ 0 & 0 & \theta_{m+\frac{1}{2}}^E \end{pmatrix}$$

- $$\mathbf{F}_{m+\frac{1}{2}} = \frac{\mathbf{F}(\bar{\mathbf{V}}_m) + \mathbf{F}(\bar{\mathbf{V}}_{m+1})}{2} - \frac{\gamma_{m+\frac{1}{2}}}{2} (\bar{\mathbf{V}}_{m+1} - \bar{\mathbf{V}}_m)$$

## Positivity of the density

- $$\theta_{m+\frac{1}{2}}^\rho = \theta_{m+\frac{1}{2}}^{\rho(1)} \theta_{m+\frac{1}{2}}$$

$$\theta_{m+\frac{1}{2}}^{\rho(1)} \leq \min \left( 1, \left| \frac{\gamma_{m+\frac{1}{2}}}{\Delta \mathbf{F}_{m+\frac{1}{2}}^\rho} \right| \rho_{m+\frac{1}{2}}^* \right)$$

## Positivity of the internal energy

- $A_{m+\frac{1}{2}} = \frac{1}{(\gamma_{m+\frac{1}{2}})^2} \left( \frac{1}{2} \left( \Delta F_{m+\frac{1}{2}}^q \right)^2 - \theta_{m+\frac{1}{2}}^{\rho(1)} \Delta F_{m+\frac{1}{2}}^{\rho} \Delta F_{m+\frac{1}{2}}^E \right)$
- $B_{m+\frac{1}{2}} = \frac{1}{\gamma_{m+\frac{1}{2}}} \left( q_{m+\frac{1}{2}}^* \Delta F_{m+\frac{1}{2}}^q - \rho_{m+\frac{1}{2}}^* \Delta F_{m+\frac{1}{2}}^E - \theta_{m+\frac{1}{2}}^{\rho(1)} E_{m+\frac{1}{2}}^* \Delta F_{m+\frac{1}{2}}^{\rho} \right)$
- $M_{m+\frac{1}{2}} = \rho_{m+\frac{1}{2}}^* E_{m+\frac{1}{2}}^* - \frac{1}{2} (q_{m+\frac{1}{2}}^*)^2$

$$\theta_{m+\frac{1}{2}} \leq \min \left( 1, \frac{M_{m+\frac{1}{2}}}{|B_{m+\frac{1}{2}}| + \max(0, A_{m+\frac{1}{2}})} \right)$$

- $\theta_{m+\frac{1}{2}}^{\rho} = \theta_{m+\frac{1}{2}}^{\rho(1)} \theta_{m+\frac{1}{2}}$ ,  $\theta_{m+\frac{1}{2}}^q = \theta_{m+\frac{1}{2}}$ ,  $\theta_{m+\frac{1}{2}}^E = \theta_{m+\frac{1}{2}}$



**A. RUEDA-RAMÍREZ, B. BOLM, D. KUZMIN AND G. GASSNER**, *Monolithic Convex Limiting for Legendre-Gauss-Lobatto Discontinuous Galerkin Spectral Element Methods*. Arxiv, 2023.

## LMP

$$\bar{v}_m^{n+1} \in I \left( \bar{v}_{m-1}^n, v_{m-\frac{1}{2}}^*, \bar{v}_m^n, v_{m+\frac{1}{2}}^*, \bar{v}_{m+1}^n \right)$$

- $v \in \{\rho, q, E\}$  conservative variable
- $\widetilde{v}_{m+\frac{1}{2}}^- \in [\alpha_m, \beta_m] := I \left( \bar{v}_{m-1}^n, v_{m-\frac{1}{2}}^*, \bar{v}_m^n, v_{m+\frac{1}{2}}^*, \bar{v}_{m+1}^n \right)$
- $\widetilde{v}_{m+\frac{1}{2}}^+ \in [\alpha_{m+1}, \beta_{m+1}] := I \left( \bar{v}_m^n, v_{m+\frac{1}{2}}^*, \bar{v}_{m+1}^n, v_{m+\frac{3}{2}}^*, \bar{v}_{m+2}^n \right)$

$$\theta_{m+\frac{1}{2}} \leq \min \left( 1, |D_{m+\frac{1}{2}}| \begin{cases} \min \left( \beta_{m+1} - v_{m+\frac{1}{2}}^*, v_{m+\frac{1}{2}}^* - \alpha_m \right) & \text{if } \Delta F_{m+\frac{1}{2}} > 0 \\ \min \left( \beta_m - v_{m+\frac{1}{2}}^*, v_{m+\frac{1}{2}}^* - \alpha_{m+1} \right) & \text{if } \Delta F_{m+\frac{1}{2}} < 0 \end{cases} \right)$$

- Smooth extrema relaxation to preserve accuracy

## Sod shock tube test case

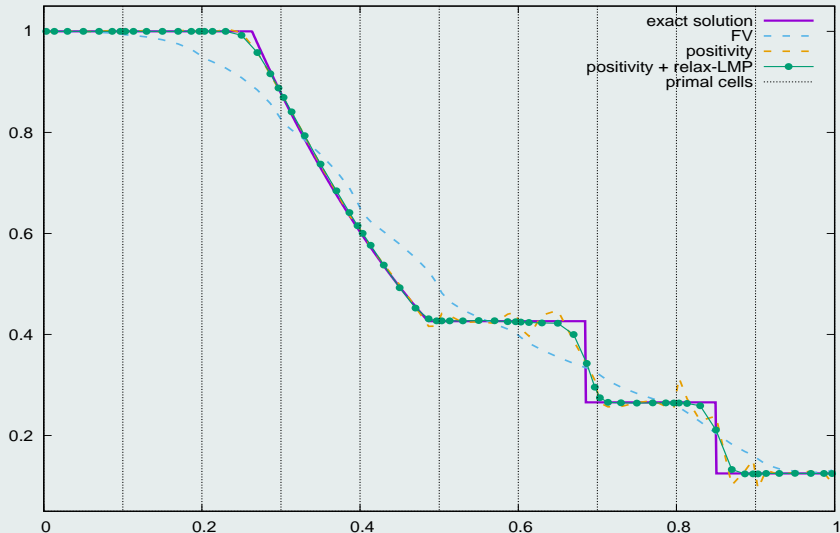
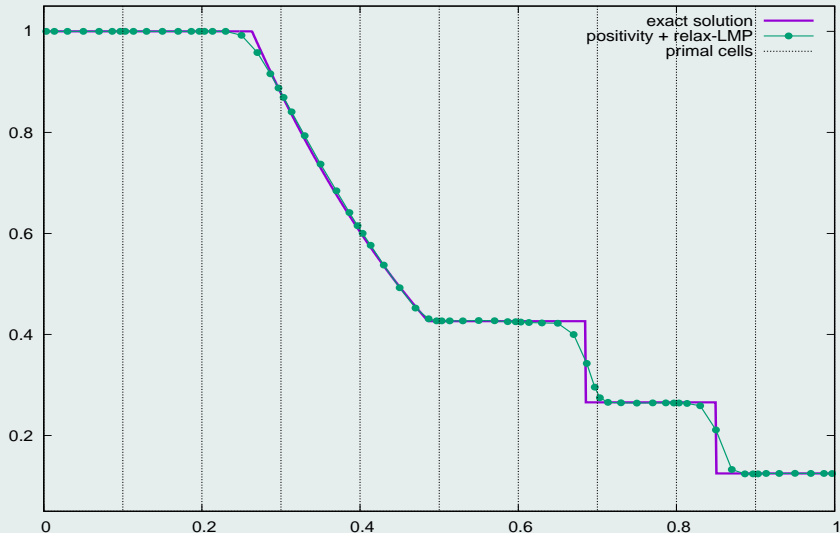


Figure :  $\mathbb{P}^6$ -DG/FV solutions on 10 cells: submean values



## Sod shock tube test case

Figure :  $\mathbb{P}^6$ -DG/FV solutions on 10 cells: submean values

# Double rarefaction test case

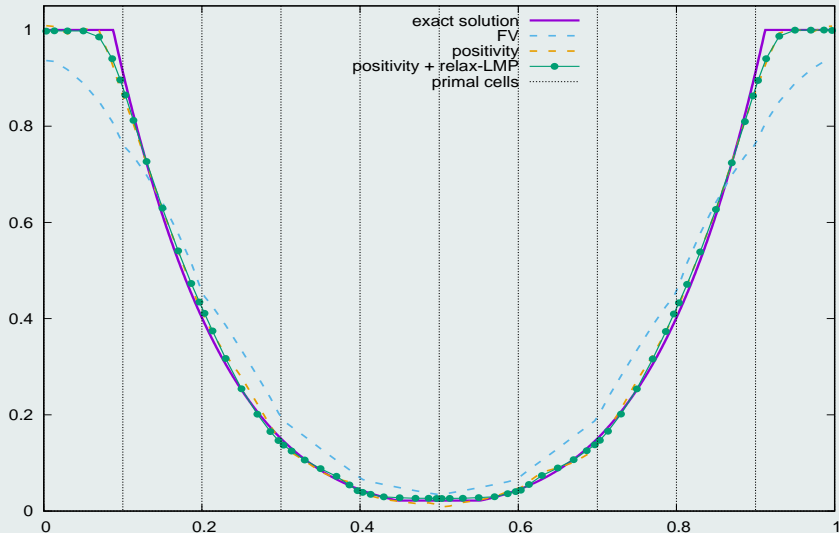
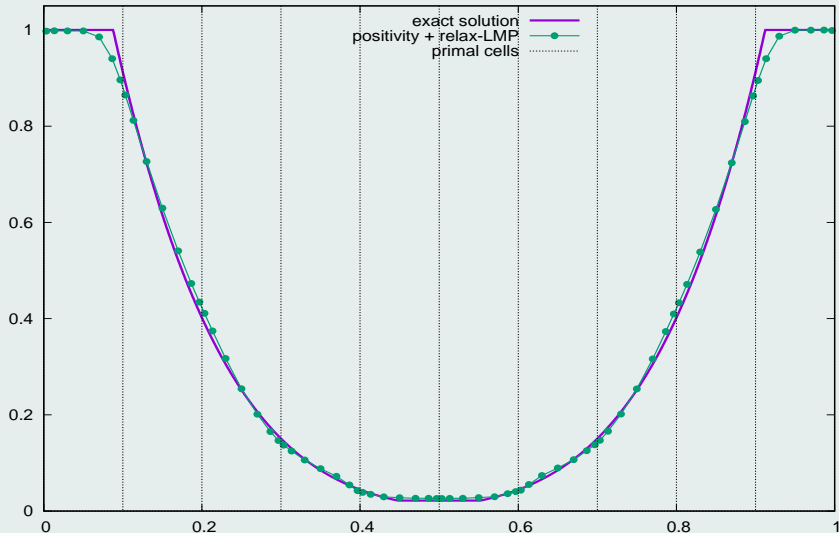


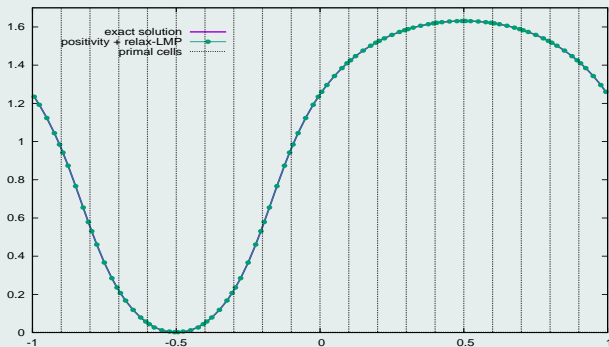
Figure :  $\mathbb{P}^6$ -DG/FV solutions on 10 cells: submean values

## Double rarefaction test case

Figure :  $\mathbb{P}^6$ -DG/FV solutions on 10 cells: submean values

## Smooth isentropic solution

$$\rho_0 = 1 + 0.9999999 \sin(2\pi x)$$



$h$	$L_1$		$L_2$	
	$E_{L_1}^h$	$q_{L_1}^h$	$E_{L_2}^h$	$q_{L_2}^h$
$\frac{1}{20}$	1.54E-5	4.01	2.04E-5	3.82
$\frac{1}{40}$	9.57E-7	4.89	1.45E-6	4.85
$\frac{1}{80}$	3.22E-8	4.84	5.00E-8	4.87
$\frac{1}{160}$	1.12E-9	-	1.71E-9	-

Table: Convergence rates computed on the pressure with a 5th-order DG/FV scheme

## Different cell subdivisions

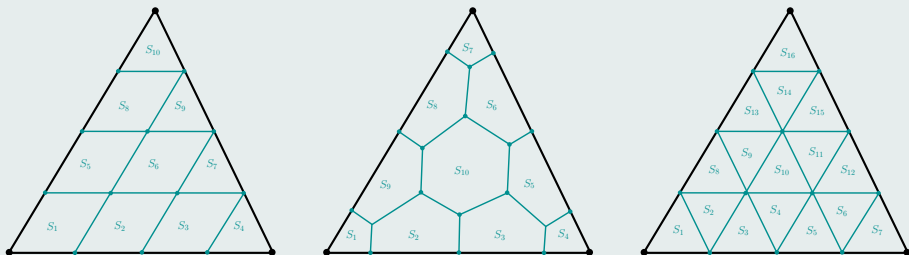
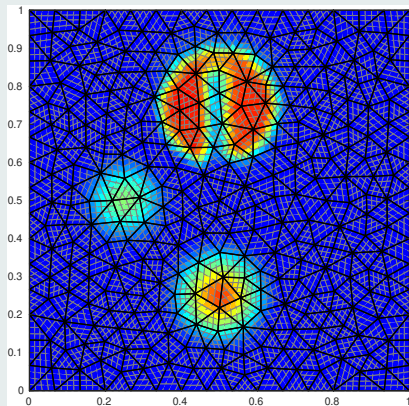
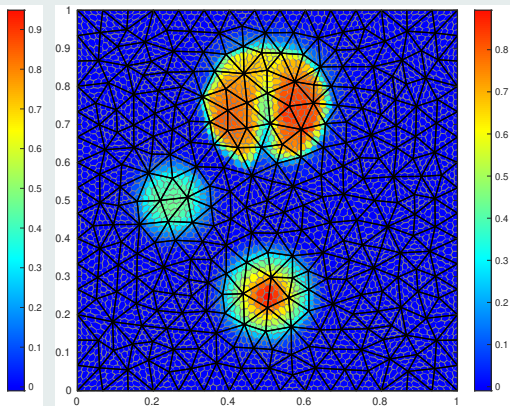
 $P^3$ 


Figure : Examples of easily generalizable subdivisions for a triangle cell

# Rotation of a composite signal after one full rotation



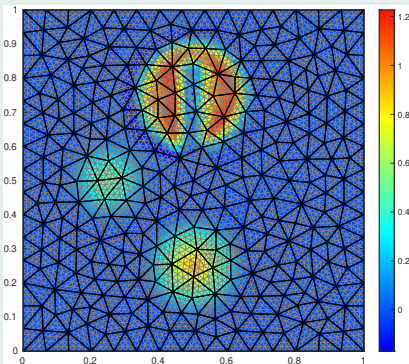
(a) Cartesian subdivision



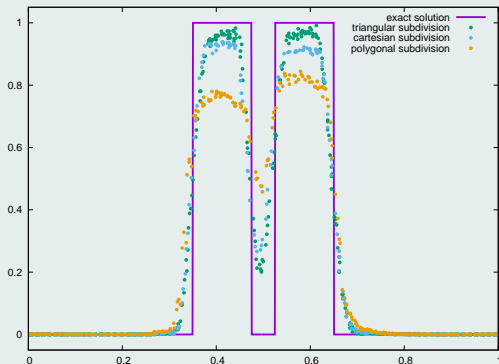
(b) Polygonal subdivision

Figure :  $\mathbb{P}^3$ -DG/FV scheme with GMP and relaxed-LMP on 576 cells: subcells mean values

# Rotation of a composite signal after one full rotation



(a) Triangular subdivision



(b) solution profiles for  $y = 0.75$

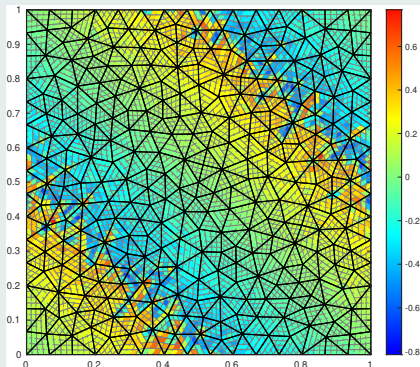
Figure :  $\mathbb{P}^3$ -DG/FV scheme with GLMP and relaxed-LMP on 576 cells

## Cell subdivision impact

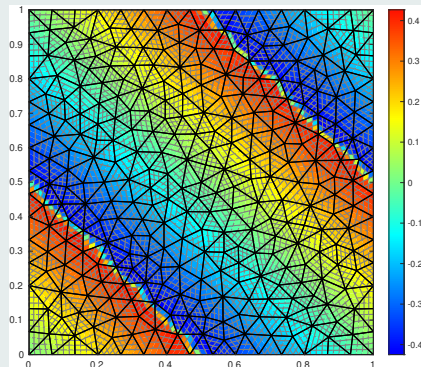
- The subdivision does have an impact on the DG/FV scheme
- Much lesser for non-linear problems

## Burgers equation

$$u_0(x, y) = \sin(2\pi(x + y))$$



(a) DG



(b) GMP + relaxed-LMP

Figure :  $\mathbb{P}^3$ -DG/FV scheme on 576 cells: subcell mean values



## Burgers equation

$$u_0(x, y) = \sin(2\pi(x + y))$$

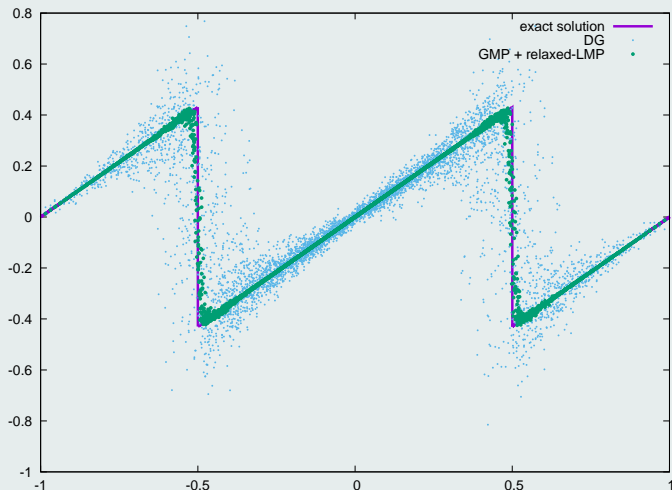


Figure :  $\mathbb{P}^3$ -DG/FV scheme with GMP and relaxed-LMP on a 576 cells mesh at  $t = 0.5$ : submean values versus  $(x + y - 1)$  coordinate

## Burgers equation

$$u_0(x, y) = \sin(2\pi(x + y))$$

(a) Solution submean values

(b) Blending coefficients

Figure :  $\mathbb{P}^3$ -DG/FV scheme with GMP and relaxed-LMP on 576 cells

***Work in progress,  
To be continued...***

***Work in progress,  
To be continued...***

## Cell subdivision: condition number of the projection matrix $P_c$

	$P^0$	$P^1$	$P^2$	$P^3$
Unif. struct. subdiv.	1	4	10.91	31.75
Non-unif. struct. subdiv.	1	4	9.52	29.28
Unif. polyg. subdiv.	1	2.87	8.73	27.89
Non-unif. polyg. subdiv.	1	2.87	8.19	26.94

**Table:** Projection matrix condition number for different orders and subdivisions